Polymer 51 (2010) 3706–3714

Contents lists available at ScienceDirect

Polymer

journal homepage: www.elsevier.com/locate/polymer

Surface hydrophilization of electrospun PLGA micro-/nano-fibers by blending with Pluronic® F-108

Rajesh Vasita [a], Gopinath Mani [b], C. Mauli Agrawal [b], Dhirendra S. Katti [a,*]

[a] Department of Biological Sciences and Bioengineering, Indian Institute of Technology – Kanpur, Kanpur-208016, Uttar Pradesh, India
[b] Department of Biomedical Engineering, University of Texas at San Antonio, San Antonio, TX, USA

ARTICLE INFO

Article history:
Received 5 March 2010
Received in revised form
8 May 2010
Accepted 22 May 2010
Available online 9 June 2010

Keywords:
Electrospinning
Poly(lactide-*co*-glycolide) (PLGA)
Pluronic®

ABSTRACT

Poly(lactide-*co*-glycolide) (PLGA) has been widely explored as scaffolds in tissue engineering. However, its hydrophobicity can adversely affect events such as protein adsorption and downstream cell adhesion in tissue engineering applications. Although surface modification techniques (high energy radiation/chemical treatment) to modify the hydrophobicity of PLGA can be useful at the macroscopic scale, their usefulness for micro-/nano-meter scale objects can be limited due to adverse affects on physical properties. Therefore, in this study we report the surface hydrophilization of electrospun micro-/nano-fiber meshes of PLGA (85:15) by blending with small quantities (0.5–2%) of a non-ionic surfactant Pluronic® F-108 (PF-108). The blended fiber meshes showed a decrease in surface contact angle when compared to pure PLGA fiber meshes demonstrating an improvement in surface hydrophilicity due to blending. This was corroborated by XPS analysis that demonstrated surface enrichment of PF-108. Thermal and mechanical studies demonstrated that blending with small quantities of PF-108 do not compromise the bulk properties of PLGA. Therefore these studies demonstrated the feasibility of hydrophilization of electrospun PLGA micro-/nano-fibers, without compromising the bulk properties (thermal and mechanical) of native PLGA.

1. Introduction

Synthetic biomaterials such as Poly(lactide-*co*-glycolide) (PLGA) have been extensively used in biomedical application because of their biocompatibility, biodegradability, mechanical strength, and amenability to modifications [1]. Tissue engineering is one such application area where PLGA has been widely used as a material to design scaffolding systems. More recently, electrospun PLGA fibers have been explored for tissue engineering applications because of their unique extra cellular matrix (ECM) mimicking non-woven micro-/nano-fibrous structure [2]. These micro-/nano-fibrous meshes of PLGA (diameter ranging from few tens of nanometers to a few microns) possess other desirable properties such as a high aspect ratio, highly porous structure (80–90% porosity), and good mechanical strength [3]. However, limited availability of hydrophilic (–COOH) functionality combined with the surface hydrophobicity of PLGA micro-/nano-fibers can compromise their interaction with proteins. It has been previously reported that increasing the surface hydrophilicity of hydrophobic materials improves cell adherence and in particular growth [4–6]. It has also been demonstrated that either extremely hydrophilic or hydrophobic surfaces are undesirable for cell attachment [4]. Rather, surfaces with moderate wettability (contact angle 40°–70°) are able to competitively adsorb cell adhesive proteins, resulting in cell attachment [5–7]. Therefore, it would be desirable to control surface hydrophobicity of PLGA micro-/nano-fibers for making them more suitable as scaffolds/substrates for cell interaction.

The past two decades have witnessed the emergence of multiple (chemical and physical) methods for improving hydrophilicity of synthetic hydrophobic polymeric surfaces [8,9]. However, only few of them have been exploited for micro-/nano-fiber modification [10]. These modification methods can be broadly classified into two categories: pre-fabrication methods and post-fabrication methods. Chemical treatment, high energy radiation treatment, and grafting of a hydrophilic polymer are post-fabrication methods that can enable surface modification without altering bulk properties [10,11]. Whereas, pre-fabrication methods such as blending and co-polymerization of hydrophilic polymers with hydrophobic polymers modify the bulk properties of polymers, which consequentially enable a change in surface properties [12]. The type and geometry of the polymeric device generally govern the choice of method for surface modification. In case of hydrophobic polymeric

* Corresponding author. Tel.: +91 512 2594028; fax: +91 512 2594010.
E-mail address: dsk@iitk.ac.in (D.S. Katti).

0032-3861/$ – see front matter © 2010 Elsevier Ltd. All rights reserved.
doi:10.1016/j.polymer.2010.05.048

micro-/nano-fibers, the hydrophobicity of the fibers limits the accessibility of chemical such as sodium hydroxide (NaOH), ethylenediamine (ED), used for surface modification as a result of which functionalization of interstitial materials in thicker 3-D meshes may not be uniform due to transport limitations [13]. Further, the small fiber diameter (i.e. high surface area) enhances the probability of bulk degradation with prolonged exposure to these solvents, thereby necessitating smaller treatment durations. Similarly, use of high energy radiations such as UV rays or gamma rays for surface modification of hydrophobic polymers is restricted to the surface of the 3-dimensional matrix (fibrous mesh) thereby limiting the surface modification along the *z*-axis (inner core). Further, the high energy radiation protocols can also result in degradation and consequential loss in physical properties of polymeric micro-/nano-fibrous systems [14]. Conversely, pre-fabrication methods such as co-polymerization and blending of hydrophilic polymers are less damaging as compared to post-fabrication modification methods, however, unlike post-fabrication methods they can lead to changes in bulk properties. PLGA, one of the extensively used co-polymers, is a product of co-polymerization of lactic acid (LA) and glycolic acid (GA). The amount of hydrophilic unit, i.e. GA in the copolymer, controls the hydrophobicity and rate of polymer degradation. However, increased hydrophilicity is associated with increased degradation rate and deterioration of mechanical properties [3]. Blending or co-polymerization of hydrophilic polymers with hydrophobic PLGA has been reported previously [15]. For example poly (ethylene glycol) has been reported for blending with PLA/PLGA [16]. The extent of hydrophilicity desired determines the percentage of PEG required in the blend. However, such blends often result in loss of mechanical strength and altered degradation rates as compared to pure PLA/PLGA [12,16]. While the aforementioned methods of modification (pre-/post-fabrication) can provide desirable outcomes for scaffolds/matrices with macro-scale dimensions (such as hydrogels), for scaffolds with micrometers to nanometers scale dimensions such as electrospun fibers, these methods can be detrimental to their physical properties. Hence, it would be desirable to have a modification method which can provide hydrophilicity to the surface of electrospun micro-/nano-fibrous meshes of PLGA while maintaining/minimally compromising the bulk/other properties of the polymer. Therefore, the purpose of this study was to impart hydrophilicity to electrospun PLGA micro-/nano-fibers by blending as small an amount as possible of a hydrophilic polymer. However, since PLGA (85:15) is a hydrophobic polymer there could be the possibility of phase separation if a hydrophilic polymer was used for blending. Hence, amphiphilic polymers such as Pluronics® could be more desirable as the hydrophobic component of Pluronic® could interact with PLGA and the hydrophilic component could impart hydrophilicity.

Pluronics® are commercially available non-ionic surfactants that have been widely used for biomedical applications including drug delivery, non-fouling, and tissue engineering applications [17–22]. It is well reported that hydrophilic Pluronics® when blended with hydrophobic polymers tends to segregate to the surface thereby modulating the surface properties of the hydrophobic polymer [23]. Hence, Pluronics with a relatively higher degree of hydrophilicity such as Pluronic® F-108 and F-127 would be more desirable. However, for this study Pluronic® F-108 was chosen over F-127 because of its relatively higher amount of EO unit (265.45 for F-108 and 200.45 for F-127) and HLB value (27 for F-108 and 22 for F-127). Here we report a pre-fabrication modification method for hydrophobic polymer PLGA 85:15 by blending with very small quantities (0.5–2.0% w/v) of Pluronic® F-108 (PF-108) which enables significant improvement in the surface hydrophilicity of PLGA micro-/nano-fiber meshes while maintaining the bulk (thermal and mechanical) properties of PLGA.

2. Materials and methods

Poly(DL-lactide-*co*-glycolide), (LA:GA – 85:15) (PLGA) with M_w 45000–70000, and pluronic® F-108 (PF-108) (82.2% EO and 17.8% PO) with M_n 14,600 were purchased from Sigma Aldrich, USA. Tetrahydrofuran (THF) and Dimethlyformamide (DMF) (HPLC grade) solvent used for electrospinning were obtained from Merck India Ltd.

2.1. Fabrication of micro-/nano-fibrous meshes

The electrospinning set-up employed in this study was indigenously designed and consisted of a syringe pump (Harvard Apparatus, USA), a high voltage power supply (Glassman High Voltage Inc., USA) and an adjustable rotatory cylindrical mandrel (length 12 cm and diameter 7.5 cm) for collection of fibers. The polymer (pure PLGA or PLGA blended with 0.5–2.0% w/v of PF-108) solution (22% w/v) prepared in THF:DMF (3:1 ratio) was loaded in a glass syringe and was pumped at a flow rate of 0.5 ml/h using a syringe pump, the distance between the needle (24 gauge) tip of the syringe and the collector mandrel was set at 29 cm, and the voltage applied was 1.2 kV/cm. Under the aforementioned condition the polymer solution ejects out of the needle tip as a jet that travel in a straight path for a short distance and then undergoes instabilities to produce a whipping motion that leads to the jet traversing a long path. While the jet traverses a long path it leads to jet stretching/thinning accompanied by solvent evaporation. The jet eventually dries to form nanofibers that were deposited on a rotating mandrel set at 300 rpm. The process resulted in the production of a non-woven fibrous mesh (non-beaded). This mesh was lyophilized for 48 h after synthesis and used for further experiments.

2.2. Scanning electron microscopy

The surface morphology and the diameter of the micro-/nano-fibers were characterized using a scanning electron microscope (SEM), (FEI Quanta 200). A representative section of the deposited micro-/nano-fibrous meshes were sputter-coated with gold and were observed under the SEM at a working distance of 10 mm and an accelerating voltage of 20 kV. The surface morphology of the fibers was observed at 2000×–4000×magnification.

2.3. Water contact angle measurement

The hydrophilicity of the nanofibrous matrix was measured by contact angle relaxation of water droplet by sessile drop method using a contact angle goniometer (Rame-hart Inc., USA equipped with CCD camera and RHI 2001 imaging software). The 1 × 1 cm freshly prepared electrospun mesh was kept under vacuum for 24 h to avoid surface contamination. The mesh was then attached to a glass slide for contact angle measurements. In each measurement, a droplet of deionized water (10 μl) was pipetted onto the membrane surface and contact angle was measured until equilibrium (i.e. no further change in contact angle). Images of the solution droplet were taken using a high speed digital camera and the values of contact angle were calculated manually from the images. The contact angle measurements were performed at 25 °C and about 65% humidity.

2.4. X-ray photoelectron spectroscopy (XPS)

XPS measurements were performed using a Kratos Axis-Ultra instrument equipped with a monochromatic Al Kα X-ray source (*E* 1486.7 eV, 225 W), a dual-anode Al/Mg X-ray gun, a hemispherical

electron energy analyzer, and a channeltron detector array. During measurement a base pressure of $<2 \times 10^{-9}$ Torr was maintained. The pass energy for the survey spectra was 160 eV and detailed spectra were taken with high resolution at 20 eV pass energy (in the case of O 1s and C 1s spectra) or at 40 eV pass energy (in the case of all other spectra). The X-ray spot size was about 800 μm and data were acquired at a normal photoelectron takeoff angle of 90°. High resolution spectra were recorded at three different spots on each sample. The binding energy (BE) values for the pure and blended nanofibrous meshes were referenced by setting the C 1s BE to 285 eV and O 1s BE to 533 eV, respectively. The BE values and atomic percentage concentrations reported here represent the average of two samples with three distinct spots on each sample along with the corresponding standard deviations. CasaXPS data analysis software was used to deconvolute the spectra and to calculate the elemental and component composition from the peak areas. To determine the amount of PF-108 on the surface of electrospun PLGA micro-/nano-fibers, monomer ratio [0.5PF-108 (C4)/PLGA (C3)] and mass ratio [0.5PF-108 (C4×M_w/PLGA (C3×M_w] were estimated from calculated intensity. To estimate the extent of PF-108 on blended micro-/nano-fibrous surfaces, 'surface enrichment' was calculated using the formula − mass ratio × 100/ percentage of PF-108 in blend.

2.5. Atomic force microscopy

Atomic force microscopy (AFM) measurements were conducted using an AFM [Molecular Imaging (MI), USA] in the non-contact, acoustic AC (AAC) mode. Advantage of AAC mode is that change in phase can be detected using topography images. Freshly prepared samples were kept under high vacuum to avoid any surface contamination and then stuck on a glass slide for imaging. Each sample was imaged at multiple locations within a scan area of 2000–5000 nm^2 for each image. All imaging was done in air at room temperature and all images were analyzed using PicoScan software.

2.6. Thermal analysis

Differential scanning calorimetry (DSC) analysis was performed on a Pyris 6 DSC (Perkin Elmer) under dynamic nitrogen atmosphere (50 ml min^{-1}), using about 10 mg of sample contained in an aluminum pan, and a heating rate of 10 °C min^{-1} from 25 to 400 °C. The DSC cell was calibrated with indium (melting point 156 °C) and zinc (melting point 419.4 °C) standards. Thermogravimetry (TG) and thermogravimetry derivative (DTG) curves were obtained using a Pyris 6 TGA (Perkin Elmer) thermogravimetric analyzer, under dynamic nitrogen atmosphere (50 ml min^{-1}), using about 10 mg of sample contained in an aluminum pan, and a heating rate of 10 °C min^{-1}, from 25 to 400 °C.

2.7. Mechanical analysis

Mechanical properties of electrospun micro-/nano-fibrous meshes made from pure PLGA and PF-108 blended PLGA were measured using a mechanical testing system (Bose Electro Force-3200, Germany) and the protocol followed was a modification of ASTM Standard D5035 and D882-09. Micro-/nano-fibrous meshes were cut into samples having a width of 5 mm, a length of 10 mm, and thickness that ranged between 0.2 and 0.4 mm. All the samples were tested under a crosshead speed of 0.1 mm/s at room temperature. Six specimens were tested in two directions of fiber collection [i.e. the machine direction (MD) and the transverse direction (TD)], and the average values were reported.

3. Results and discussion

3.1. Fiber preparation and characterization

Most tissues consist of a collagen based fibrous extra cellular matrix (ECM) with fiber/fibril diameter ranging from a few nanometers to a few tens of micrometers. The ability to produce/fabricate as well as modulate fiber diameters in the aforementioned range using the electrospinning technique has lead to wide-spread exploration of electrospun micro-/nano-fibers as ECM mimicking scaffolding systems for tissue engineering applications. Electrospun micro-/nano-fibers fabricated using PLGA 85:15 due to the higher LA content possess good mechanical strength and relatively longer degradation profiles which makes them desirable for bioactive agent delivery and tissue engineering applications. However, the higher LA content also imparts hydrophobicity to the micro-/nano-fiber surfaces and can adversely affect protein adsorption and the conformation of adsorbed proteins. Therefore, in the current study PLGA 85:15 was blended with 0.5–2.0% of PF-108 with the objective of imparting hydrophilicity to the electrospun PLGA micro-/nano-fibrous meshes. The ratio of hydrophilic ethylene glycol (EO) to hydrophobic propylene glycol (PO) in the PF-108 imparts a distinct hydrophilic-hydrophobic balance to the co-polymers [17]. PF-108 (with 82.2% EO and 17.8% PO) was chosen for this study with the premise that the 82.2% EO units would provide for the hydrophilicity, whereas, the 17.8% of PO units would facilitate its miscibility in hydrophobic PLGA. Micro-/nano-fibers fabricated by electrospinning blends of PLGA and PF-108 formed non-woven fibriller mesh structures as shown in Fig. 1. Fiber orientation was random with an average fiber diameter of 800 nm and a diameter range of 200–1000 nm. Scanning electron micrographs in Fig. 1 revealed a smooth morphology and random fibrous structure with no significant difference in morphology (at 2000× magnification) between blended and unblended (inset) micro-/nano-fiber meshes.

3.2. Water contact angle (WCA) measurement

Pluronics® are block co-polymers that exhibit a wide range of hydrophobic/hydrophilic properties [hydrophilic–lipophilic balance value (HLB)] depending on the molar ratio of the hydrophilic EO units and the hydrophobic PO units. PF-108 used in this study contains 82.5% EO units (number of EO units 265.45); with an HLB value of 27 which makes it a hydrophilic polymer. Therefore in this study, contact angle measurements were performed to understand the influence of PF-108 enrichment on micro-/nano-fiber surfaces and as a consequence on the overall hydrophilicity of the micro-/nano-fiber meshes. Contact angle of water droplets on micro-/nano-fibrous meshes was recorded at 10 s intervals from 10 to 140 s and a plot of contact angle Vs time (Fig. 2) was generated to understand the change in contact angle with time. A significant decrease in contact angle was observed even with the smallest concentration (i.e. 0.5%) of PF-108 blended PLGA micro-/nano-fibrous meshes as compared to pure PLGA micro-/nanofibrous meshes. The rate of water drop spreading was almost negligible for pure PLGA meshes. However, for blended PLGA meshes there was a gradual drop in water contact angle till 1.0% PF-108 blending, whereas, 1.5% and above demonstrated rapid spreading of water droplet. In a previous study by Kiss et al. wherein blending of pluronic PE 6800 (80% EO) into PLGA (75:25) thin film was studied and their results demonstrated that increasing PE 6800 concentration (1–9.1 wt.%) into PLGA thin films caused a decrease in contact angle on the film [24]. In the current study, where, micro-/nano-fibrous meshes were used in place of films, similar results were observed, wherein increasing PF-108 content from 0.5 to 2.0% (w/v) significantly increased the hydrophilicity of the blended

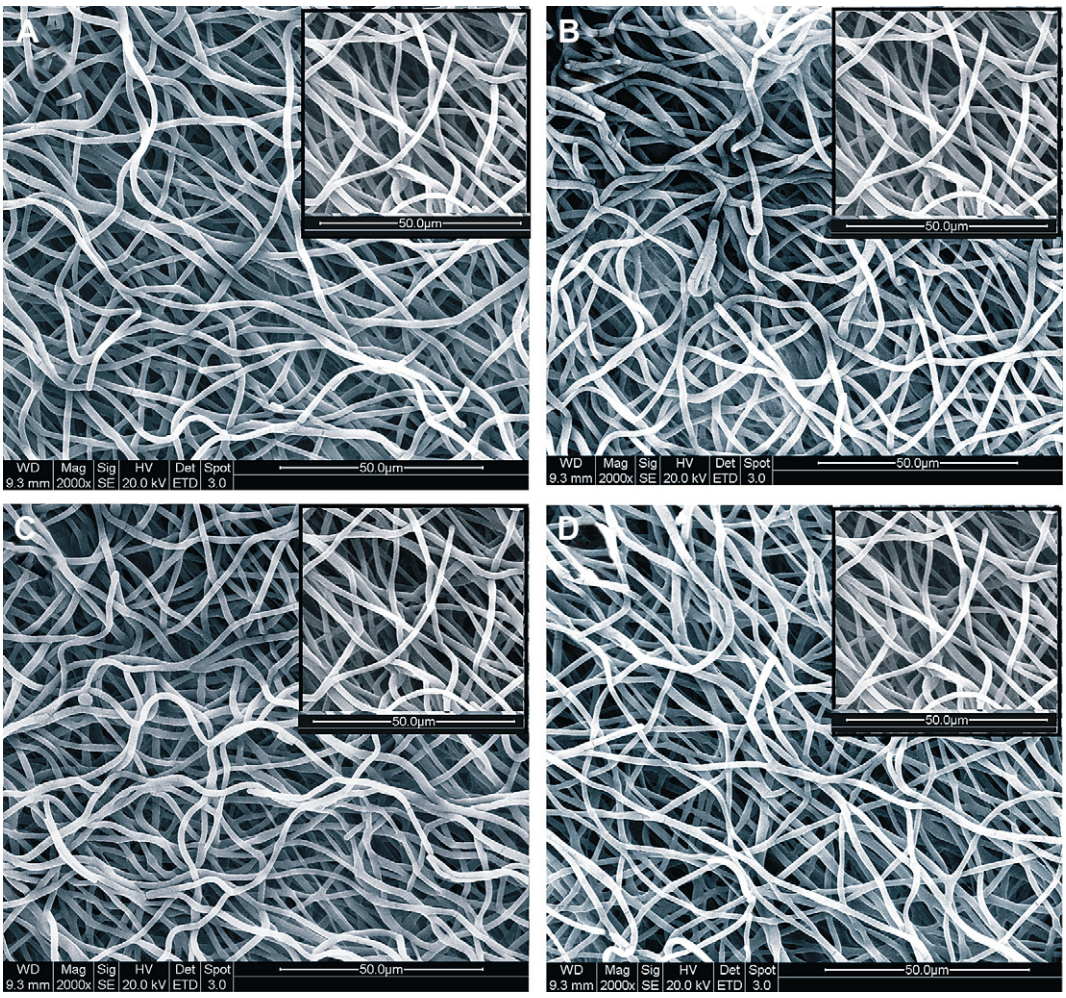

Fig. 1. Scanning electron micrographs of PF-108 (0.5–2.0% w/v) blended and unblended PLGA micro-/nano-fibrous meshes. (A) PLGA blended with 0.5% PF-108, (B) PLGA blended with 1.0% PF-108, (C) PLGA blended with 1.5% PF-108, (D) PLGA blended with 2.0% PF-108. The inset in all images is a micrograph of fiber meshes of pure PLGA. Scale bar in all images and inset images is 50 μm.

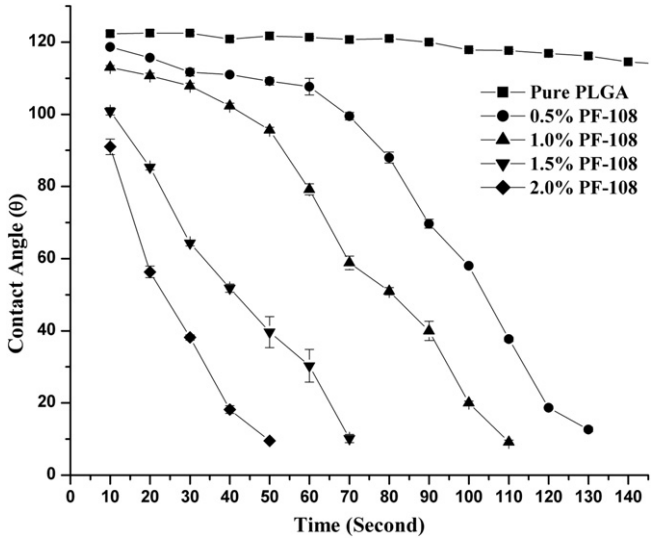

Fig. 2. Dynamic water contact angles (Θ) on PF-108 blended (0.5–2.0% w/v) and unblended PLGA micro-/nano-fibrous meshes. (■) Pure PLGA (●) PLGA blended with 0.5% PF-108, (▲) PLGA blended with 1.0% PF-108, (▼) PLGA blended with 1.5% PF-108, (◆) PLGA blended with 2.0% PF-108. Standard deviations of contact angles did not exceed ±1.5° for $n = 4$.

micro-/nano-fibrous meshes. In the study involving thin films of blends of pluronic and PLGA by Kiss et al. it was observed that blending lead to a drop in contact angle, however, the drop (~80°–~44°) was not as significant as the one observed in the present study (~120°–~10°) although the PLGA used for the present study was more hydrophobic (LA:GA – 85:15 as against LA:GA – 72:25/50:50 used in the study by Kiss et al.).

It is speculated that the increase in hydrophilicity in the micro-/nano-fiber meshes could be because of the possible hydrophobic interaction between the $-CH_3$ groups of PLGA and the $-CH_3$ groups of PF-108 (Fig. 3) which restrict the integration of EO monomers into the PLGA polymer chains thereby projecting them towards the surface. Like PF-108, the Pluronic family has various members with different EO/PO ratio and HLB which can be exploited for similar application to modulate the surface hydrophilicity/hydrophobicity of PLGA based micro-/nano-fibrous systems.

3.3. Surface composition by X-ray photoelectron spectroscopy

The WCA study demonstrated a decrease in contact angle with increase in extent of blending of PF-108 thereby indicating a change in surface composition. Therefore, XPS studies were performed to analyze the surface composition of blended micro-/nano-fibrous meshes. XPS analysis was performed on PF-108 (0.5–2.0%) blended

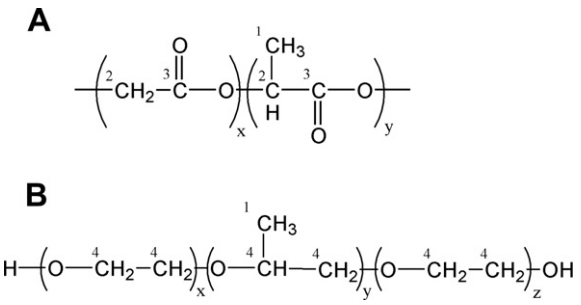

Fig. 3. Chemical formula of repeating unit of (A) PLGA composed of lactic acid (LA) and glycolic acid (GA) blocks. x: Number of monomer units of GA; y: Number of monomer units of LA. (B) PF-108 composed of Ethylene glycol (EO) and Propylene glycol (PO) blocks. x & z: Number of monomer units of EO. y: Number of monomer units of PO. (Numbers on atoms indicate types of carbons in different chemical environments producing Cls electrons at various binding energies in XPS spectra).

PLGA micro-/nano-fibrous meshes with pure PLGA micro-/nano-fibrous mesh and thin film of pure PF-108 as the controls. All electrospun samples were collected on a glass surface and the absence of a Si peak from the glass surface suggested the presence of a continuous micro-/nano-fibrous cover on the glass surface. The XPS spectra (Fig. 4) of pure PLGA, pure PF-108 (thin film) and PF-108 blended PLGA micro-/nano-fibrous meshes were used for further quantification. The overall carbon and oxygen composition of all samples are presented in Table 1. The presences of an increased percentage of total carbon atoms (higher carbon to oxygen ratio in PF-108 as compared to PLGA) and decreased percentage of total oxygen atoms on blended samples indicated the possible presence of PF-108 on the surface of the micro-/nano-fibers. The presences of increased percentage of PF-108 carbon (C4) as compared to PLGA carbons (C1–C3) demonstrated the presences of PF-108 on the surface of the micro-/nano-fibers. Fig. 3 shows the chemical structure of both polymers (PLGA and PF-108) with carbon numbers that were referred for XPS studies. Considering the chemical structure of the copolymer PLGA, peaks at 288.9 eV and 287.0 eV were assigned

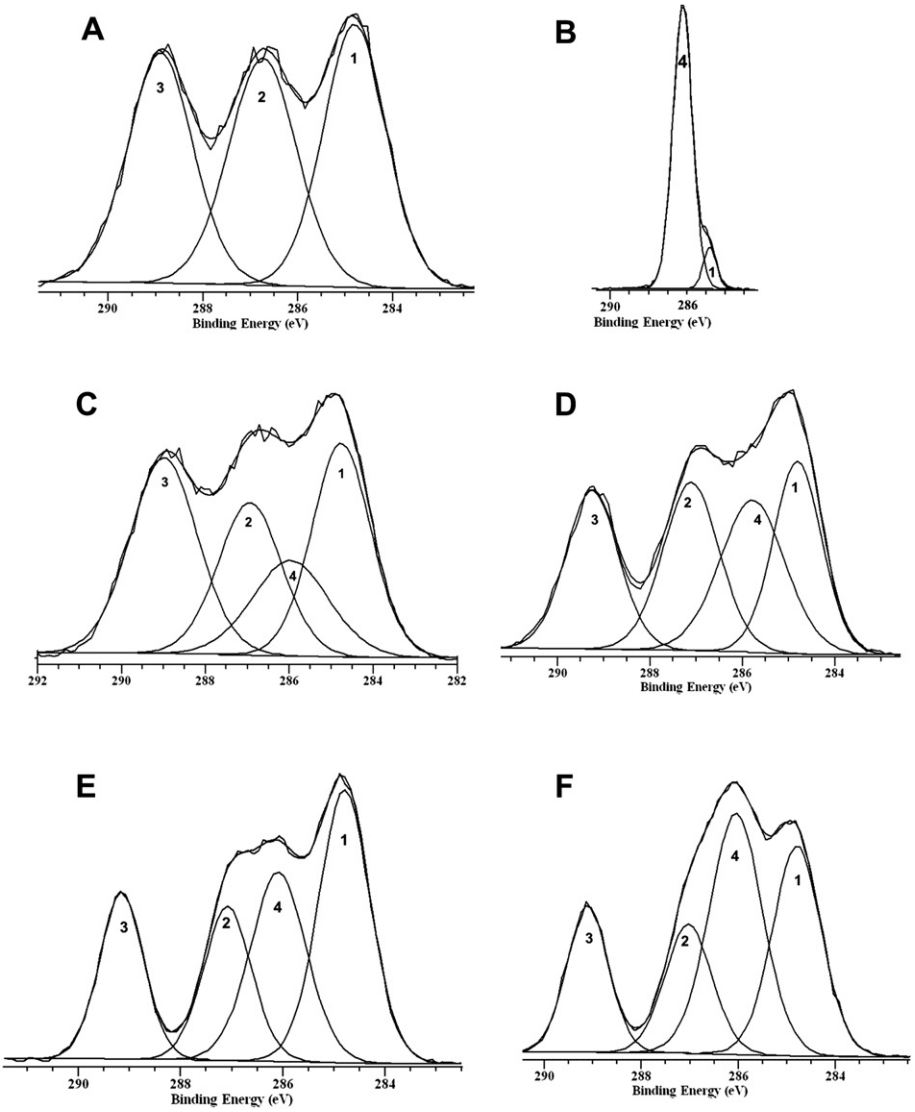

Fig. 4. Deconvoluted carbon XPS signals of PF-108 (0.5–2.0% w/v) blended and unblended PLGA micro-/nano-fibrous meshes. (A) Pure PLGA, (B) Pure PF-108, (C) PLGA blended with 0.5% PF-108, (D) PLGA blended with 1.0% PF-108, (E) PLGA blended with 1.5% PF-108, (F) PLGA blended with 2.0% PF-108. Synthetic Cls components correspond to the aliphatic carbon (1) at 284.8 eV, the carbon connected to (2) and constituting ester group (3) of PLGA at 287.0 and 288.9 eV respectively, and the etheric carbon of PF-108 additive (4) at 286.2 eV.

Table 1
Surface Compositions of PLGA micro-/nano-fibrous meshes blended with various concentrations (0.5–2.0% w/v) of PF-108. The carboxylic carbon (O–C=O) and ether carbon (C–O) components of the C1s peak in the XPS spectra correspond to PLGA and PF-108 respectively. The compositions of the surface layers, expressed as monomer ratio, mass ratio, and enrichment of PF-108 on the surface layer compared to the bulk, are also displayed.

Micro-/nano-fiber mesh type	XPS data (atomic%)						Mono-mer Ratio[a]	Mass Ratio[a]	Surface enrichment of PF-108
	Total C1s at %	Total O1s at %	C–H (1) 284.8 eV	C–O (2) 287.0 eV	C=O (3) 288.9 eV	C–O (4) 286.2 eV			
Pure PLGA mesh	56.8 ± 7.2	43.2 ± 7.2	37.5 ± 5.9	29.5 ± 3.3	33.0 ± 7.1	–	–	–	–
PLGA blended with 0.5% PF-108	64.4 ± 1.2	35.6 ± 1.2	32.2 ± 2.6	15.7 ± 8.2	35.4 ± 5.3	16.7 ± 2.8	0.23 ± 0.02	0.155	31
PLGA blended with 1.0% PF-108	63.1 ± 3.1	36.9 ± 3.1	25.9 ± 0.7	25.3 ± 0.5	24.2 ± 1.4	24.6 ± 2.1	0.51 ± 0.03	0.335	33.5
PLGA blended with 1.5% PF-108	67.5 ± 0.0	32.5 ± 0.0	31.2 ± 6.4	22.1 ± 4.7	21.6 ± 4.1	25.1 ± 2.5	0.58 ± 0.07	0.383	25.5
PLGA blended with 2.0% PF-108	66.2 ± 0.5	33.8 ± 0.5	28.1 ± 1.5	19.5 ± 3.2	17.8 ± 0.8	34.6 ± 2.5	0.97 ± 0.03	0.641	32.05
Pure PF-108 film	71.6 ± 0.9	28.4 ± 0.9	10.1 ± 0.9	–	–	89.9 ± 0.9	–	–	–

[a] PF-108/PLGA.

to the carboxylic group (C=O) carbon (C3) and to the neighboring (C–O) carbon (C2) in the backbone of the polymer respectively. The binding energy of PF-108 ether carbon (C–O) was 286.2 eV (C4) and was found to be lower than the corresponding ether carbon of PLGA (C2). In accordance with previously reported data [24], we observed a difference of 0.8 eV between the binding energies of C–O from PLGA and C–O from PF-108, which enables an easy distinction of the two polymers. Therefore, further quantification was based on the easily attributable C=O (C3) and C–O (C4) functionality and their binding energy. Taking into consideration that one monomeric unit of PF-108 contains two ether carbon atoms, monomer and mass ratios of PLGA and PF-108 were estimated from the measured intensities (Table 1). To express the PF-108 content on the surface (i.e. mass ratio, monomer ratio and surface enrichment) the average molecular weight of a single monomer unit was used (PLGA = 69.9, PF-108 = 46.5). A significant presence of C–O from PF-108 as compared to C=O from PLGA (mass ratio and monomer ratio) on the surface of micro-/nano-fibrous meshes demonstrates the presence of PF-108 on the surface and is probably the reason for increased surface wettability of the blended micro-/nano-fibrous meshes. A constant surface enrichment value of PF-108 indicated that surface saturation of PF-108 probably occurred at lower concentrations i.e. 0.5 and 1.0%, thereby indicating the possibility of the presence of excess PF-108 (at >1% blending) in the bulk of micro-/nano-fibers. In a previous study by Shi et al. where they studied molecular level surface structures of PF-127 on a hydrophobic polymer (polyethersulfone – PES), it was demonstrated that when small amounts of PF-127 were blended with PES (0–5%), PF-127 did segregate to the surface of PES, however, it did not provide complete coverage of the PES surface [23]. The reason provided by the authors is that the EO unit of PF-127 tends to stay in the PES matrix in order to avoid unfavorable interactions with air. Similarly, in this study with an increase in the concentration of PF-108 the enrichment ratio on PLGA surfaces did not change significantly. It is speculated that this was probably because of the thermodynamically favorable interaction of the EO unit of PF-108 with PLGA.

Therefore, the XPS analysis demonstrated the presence of PF-108 on the fiber surface and that the extent of PF-108 present on the surface played an important role in governing the wettability characteristics of the blended micro-/nano-fibrous meshes.

3.4. Polymeric phase behavior by AFM

The availability of multiple block co-polymers can cause nano/micro-scale phase separation within the bulk as well as surface of the electrospun polymeric micro-/nano-fibers. The presence of such separated phases can be visualized using an AFM if the blended polymers are present in sufficient concentration. Such phase separation properties often result in deterioration of mechanical properties and hence can be undesirable. In this study, the possibility of phase separation in the binary block copolymer blend, was analyzed using the tapping mode of AFM. AAC mode (tapping mode) AFM experiments were performed to enable phase imaging of the micro-/nano-fibers. Single elctrospun micro-/nano-fibers of pure PLGA (Fig. 5A), 2% PF-108 blended PLGA (Fig. 5B) and 50% PF-108 blended PLGA (Fig. 5C) were scanned vertically and horizontally for identification of polymeric phase separation. The phase images obtained from the AFM of pure PLGA and PLGA blended with 2.0% PF-108 do not provide a strong contrast between the different domains (i.e. absence of sudden change in intensity) and hence indicated a homogenous distribution of PF-108 on the PLGA fiber surface. However, when PLGA was blended with 50% (w/v) PF-108 (Fig. 5C), a strong contrast (depicted by black arrow) was observed between different domains. This is also evident from the intensity plot at the bottom of the topographical scan in Fig. 5A, B, C, wherein, the change in intensity in 5A and 5B was not significant, however, the change in intensity in 5C was significant (depicted by blue arrow). Therefore, it can be concluded that solvent compatibility and the relatively small concentrations of PF-108 (0.5–2.0%) used in these experiments do not cause a phase separation on the surface of the electrospun blended polymeric micro-/nano-fibers. Although the tapping mode AFM analysis demonstrated the absence of phase separation on the surface of micro-/nano-fibers, the possibility of phase separation in the bulk remained unresolved. Therefore, to understand the influence of blending of PF-108 on the bulk properties of the micro-/nano-fibers, thermal and mechanical analyses were performed.

3.5. Thermal analysis

The thermal behavior of polymeric micro-/nano-fiberous meshes can be directly related to their physico-chemical properties such as polymeric phase separation, percentage crystallinity, and polymeric chain interaction. Hence, the thermal properties of PLGA and the PLGA/PF-108 blends were investigated by DSC and TGA. The DSC thermograms showed two thermal events (Table 2 and Fig. 1 – Supplementary information) for both PLGA alone and PLGA blended with PF-108 (0.5%–2.0%) micro-/nano-fibrous meshes. The thermograms demonstrated that the glass transition temperature dropped from 54.98 °C for pure PLGA micro-/nano-fibrous meshes to 49.21–52.37 °C for the blended samples (Table 2 and Fig. 1A – Supplementary data). The small decrease in T_g in the blended PLGA samples could be attributed to the chain relaxation/reorganization in PLGA due to the surfactant properties of PF-108. Similarly, the latent heat of melting dropped from (–)232.45 J/g for pure PLGA micro-/nano-fibrous meshes to (–)346.42 - (–)392.78 J/g for blended samples (Table 2 and Fig. 1B – Supplementary data). Therefore, this study demonstrated that the T_g of PLGA was not

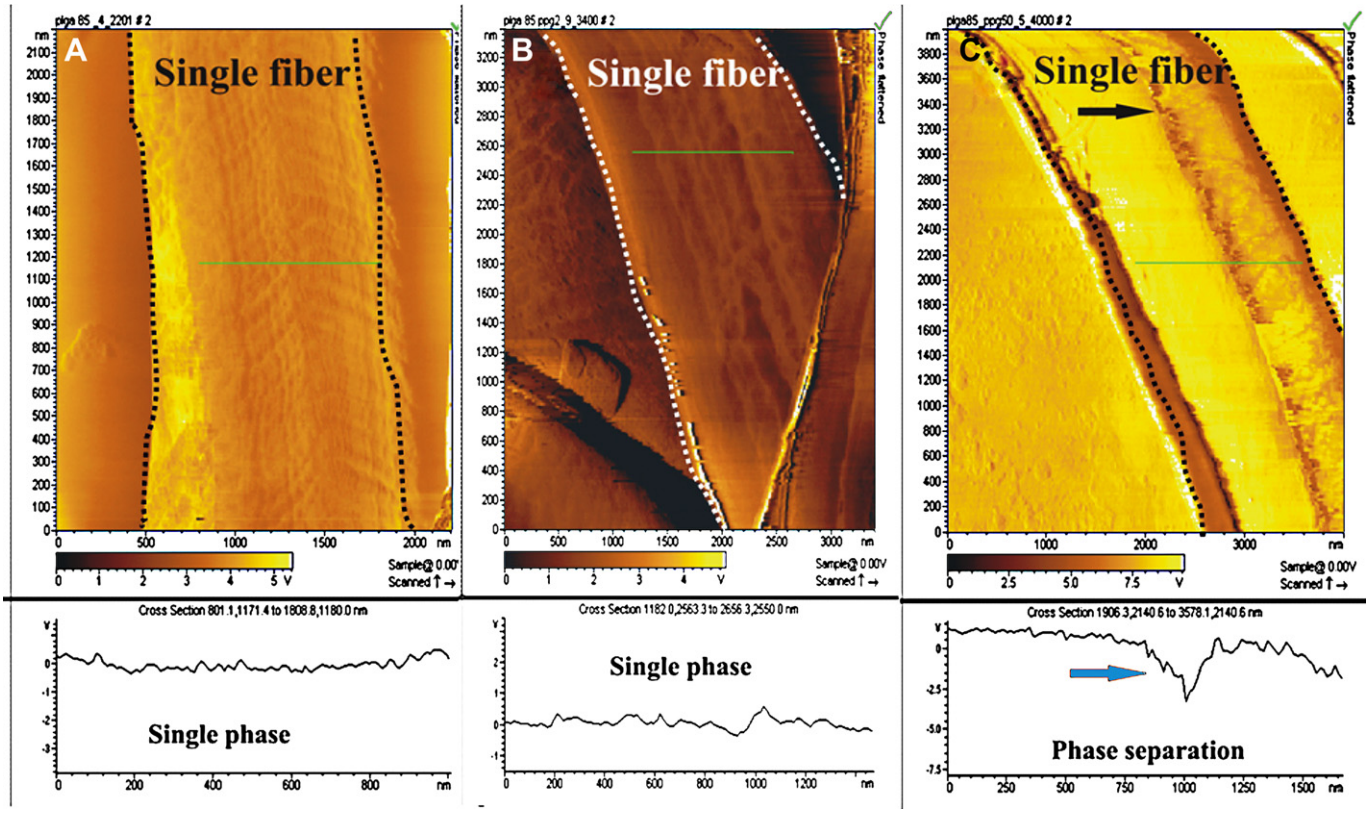

Fig. 5. Tapping mode AFM images of PF-108 blended and unblended PLGA single micro-/nano-fiber surface. (A) Pure PLGA (B) PLGA blended with 2.0% PF-108 (C) PLGA blended with 50% PF-108. The fiber in all images (A, B & C) is oriented approximately vertical to the profile line (green) and the dotted lines indicate the boundary of the scanned fiber. Change in phase is indicated by arrow in 5C (black arrow – topographical image and blue arrow – phase window). (For interpretation of the references to colour in this figure legend, the reader is referred to the web version of this article.)

significantly influenced, whereas, the latent heat of melting increased significantly when blended with small concentrations (≤2.0%) of PF-108. The possible reason for an increase in the latent energy requirement with increasing concentration of PF-108 could be polymer chain interactions between PLGA and PF-108. It can be speculated that after enrichment of PF-108 on the surface, it was probably being introduced into the bulk of the blended micro-/nano-fibers, where it could either be changing the orientation of packing of PLGA polymeric chains or causing a non-ionic interaction with PLGA molecules (phase mixing). It is further speculated that the possibility of interaction between EO units of PF-108 and GA units of PLGA, and, between PO units of PF-108 and LA units of PLGA are thermodynamically favorable and thereby could increase the probability of phase mixing. This speculation is based on a previous study by Park et al. that demonstrated a favorable interaction between PLA and the PO units of PF-108 [25]. Furthermore, from the thermogravimetry analysis (TGA/DTG) data it was evident that all samples (blended and unblended PLGA) had a similar thermal behavior (Fig. 2 – Supplementary data) in that they showed a single stage thermal degradation within a relatively narrow temperature range (338–354 °C). However, additions of PF-108 lead to a slight decrease in the melting temperature of PLGA, resulting in a small drop in thermal stability of blended PLGA as compared to pure PLGA micro-/nano-fibrous meshes. In the range of 221–375 °C, the melting and thermal decomposition of all samples continued with the elimination of carbonaceous material. The amount of residual mass after thermal degradation gradually increased from unblended to blended meshes. The PF-108 blended samples showed a residual weight of approximately 1.6%–10.2% of the original weight, whereas, it was approximately 1.07% for pure PLGA micro-/nano-fibrous meshes. Since the reported T_m of PF-108 is ~390 °C, its increasing concentration into blends could be

Table 2
Thermal analysis data of PF-108 (0.5%–2.0% w/v) blended and unblended PLGA micro-/nano-fibrous meshes. The differential scanning calorimetry (DSC) study provided the glass transition temperature (T_g) and latent heat of melting, whereas, the thermogravimetry (TGA) analysis study provided melting temperature (T_m) and percentage weight loss for PF-108 blended and unblended meshes.

Micro-/nano-fiber mesh type	DSC		TGA	
	Glass transition temperature. T_g(°C)	Latent heat of melting (J/g)	Melting temperature T_m (°C)	Percentage weight loss of polymer
Pure PLGA mesh	54.9	232.4	354.2	98.3
PLGA blended with 0.5% PF-108	52.4	346.4	351.4	96. 9
PLGA blended with 1.0% PF-108	49.3	333.6	344.3	92.9
PLGA blended with 1.5% PF-108	49.2	392.7	343.0	91.5
PLGA blended with 2.0% PF-108	51.1	386.6	338.5	89.7

Table 3
Mechanical properties of PF-108 (0.5%–2.0% w/v) blended and unblended PLGA micro-/nano-fibrous meshes.

Micro-/nano-fiber mesh type	Tensile modulus (MPa)	Tensile strength (MPa)	Yield stress (MPa)	Elongation (%)
Pure PLGA mesh	27.82	1.03	1.07	39.95
PLGA blended with 0.5% PF-108	66.16	1.68	1.27	57.75
PLGA blended with 1.0% PF-108	115.75	2.57	2.21	59.1
PLGA blended with 1.5% PF-108	144.68	4.20	3.53	60.12
PLGA blended with 2.0% PF-108	91.89	2.63	3.22	64.01

a possible reason for increase in residual mass. Therefore, this study demonstrated that incorporation of PF-108 in small concentrations (0.5–2.0%) does not cause a significant change in the thermal properties of the micro-/nano-fibrous meshes. The absences of a significant change in thermal transition values also indicated that phase separation was probably not occurring in the bulk of the micro-/nano-fibrous meshes as well.

3.6. Mechanical analysis

In order to better understand the influence of blending of small quantities of PF-108 on a bulk property such as mechanical strength of PLGA micro-/nano-fibrous meshes, tensile testing was performed. Some of the characteristic values obtained from load deformation curves are summarized in Table 3. It was observed that all PF-108 blended samples demonstrated an improvement in mechanical properties (modulus and strength) when compared to pure PLGA micro-/nano-fibrous meshes. The tensile modulus increased approximately 2.5–5 folds with an increase in the concentration of PF-108 in the blended PLGA micro-/nano-fibrous meshes. Similarly, a gradual increase (1.2–3-fold) in yield stress with increasing concentration of PF-108 demonstrated an increase in elastic deformation limit as compared to pure PLGA. While the blending of PF-108 led to an increase in the tensile modulus of the blended micro-/nano-fibrous meshes, it also led to an increase in percentage elongation of the samples. The PF-108 blended PLGA meshes demonstrated 57–64% elongation as compared to 39.95% elongation of unblended PLGA mesh. A previous study that reported blending of PEG with PLA and PLGA have demonstrated that increasing concentration (20–50%) of PEG into the blended systems, led to a drop in modulus of the fiber meshes [12]. This indicated that lower concentration of blending polymer (i.e. hydrophilic polymer) is probably desirable from the point of view of mechanical properties. However, in this study the extent of PF-108 used for blending (0.5–2.0% w/v of PLGA) is very small when compared to previous studies. Although the extent of PF-108 was very small it still enabled an improvement in the mechanical properties along with a significant change in surface properties of the electrospun micro-/nano-fibrous meshes. The increase in tensile properties i.e. young modules, ultimate tensile strength and percentage elongation of blended fibers indicated that blending concentration range of PF-108 (0.5–2.0% w/v) probably enriched the surface as well as the bulk of the micro-/nano-fibrous meshes where it was possibly causing an interaction with PLGA molecules and altering packing of polymeric chains. It is speculated that this improved polymeric chain arrangement was probably causing the enhancement in mechanical properties. Hence, this study demonstrated that mechanical properties of PLGA micro-/nano-fibrous meshes can be altered by blending of small concentrations of PF-108 (0.5%–2.0%).

4. Conclusions

Blending has been reported as a pre-fabrication technique for bulk and surface modification of electrospun micro-/nano-fibrous meshes [12]. This study demonstrated that blending with small quantities (0.5–2.0% w/v) of a hydrophilic polymer PF-108 (an amphiphilic polymeric surfactant) with hydrophobic PLGA can cause a significant increase in surface wettability of electrospun blended fibers without adversely affecting the bulk properties of PLGA micro-/nano-fibrous meshes. The improved surface wettability of the blended micro-/nano-fibrous meshes was attributed to the presence of hydrophilic PF-108 on the micro-/nano-fiber surface as evidenced by contact angle determinations and XPS analysis. Increasing concentration of PF-108 demonstrated a significant decrease in contact angle on micro-/nano-fiber mesh surfaces. XPS analysis revealed that increasing the extent of blended PF-108 does not lead to an increase in the surface enrichment ratio and thereby indicated the possibility of incorporation/dispersion of PF-108 into the bulk of micro-/nano-fibrous meshes. AFM analysis of micro-/nano-fiber surfaces for possible phase separation due to blending of different block co-polymers revealed the absence of any phase separation at low concentrations ($\leq$2.0%) of blending. Thermal analysis of blended micro-/nano-fibrous meshes showed a small decrease in T_g values and a significant increase in the latent heat of melting which demonstrated the plasticizing properties of PF-108 and the possibility of polymeric chain interactions between PF-108 and PLGA. The mechanical studies demonstrated improved tensile properties (modulus and strength) by incorporation of small concentrations of PF-108 into PLGA micro-/nano-fibrous meshes. Therefore, these studies demonstrated that blending of PLGA with small concentration of PF-108 ($\leq$2.0%) can be an effective pre-fabrication technique for modulating surface hydrophobicity of electrospun micro-/nano-fibrous meshes while maintaining (thermal properties) or improving (mechanical properties) the bulk properties of the meshes. Moreover, by varying the type and concentration of Pluronic® used for blending with PLGA it may be possible to modulate the surface properties of electrospun PLGA micro-/nano-fibrous meshes without significantly influencing the bulk properties of PLGA micro-/nano-fibers.

Acknowledgment

The authors would like to thank the Department of Biotechnology, Government of India for funding this research work. The authors would like to thank Department of Science and Technology unit on Nanoscience at IIT Kanpur for providing SEM, AFM and Goniometer facility and Dr. V. Chandrasekhar, IIT Kanpur for providing the DSC facility. RV would like to thank Council of Scientific and Industrial Research (CSIR), India for his research fellowship.

Appendix. Supplementary data

Supporting information associated with this article can be found, in the online version, at doi:10.1016/j.polymer.2010.05.048.

References

[1] Nair LS, Laurencin CT. Prog Polym Sci 2007;32:762–98.
[2] Toh YC, Ng S, Khong YM, Zhang X, Zhu YJ, Lin PC, et al. Nano Today 2006;1:34–43.

[3] Shin HJ, Lee CH, Cho IH, Kim YJ, Lee YJ, Kim IA, et al. J Biomater Sci Polym Ed 2006;17:103–19.
[4] Lee JH, Khang G, Lee JW, Lee HB. J Colloid Interface Sci 1998;205:323–30.
[5] Arima Y, Iwata H. J Mater Chem 2007;17:4079–87.
[6] Arima Y, Iwata H. Biomaterials 2007;28:3074–82.
[7] Wan Y, Chen W, Yang J, Bei J, Wang S. Biomaterials 2003;24:2195–203.
[8] Vasita R, Shanmugam K, Katti DS. Curr Top Med Chem 2008;8:341–53.
[9] Goddard JM, Hotchkiss JH. Prog Polym Sci 2007;32:698–725.
[10] Yoo HS, Kim TG, Park TG. Adv Drug Delivery Rev 2009;61:1033–42.
[11] Khang G, Choee JH, Rhee JM, Lee HB. J Appl Polym Sci 2002;85:1253–62.
[12] Bhattarai SR, Bhattarai N, Viswanathamurthi P, Yi HK, Hwang PH, Kim HY. J Biomed Mater Res A 2006;78A:247–57.
[13] Croll TI, O'Connor AJ, Stevens GW, Cooper-White JJ. Biomacromolecules 2004;5:463–73.
[14] Yixiang D, Yong T, Liao S, Chan CK, Ramakrishna S. Tissue Eng Part A 2008;14:1321–9.
[15] Dailey LA, Kissel T. Drug Disc Today Tech 2005;2:7–13.
[16] Kim K, Yu M, Zong XH, Chiu J, Fang DF, Seo YS, et al. Biomaterials 2003;24:4977–85.
[17] Kabanov AV, Lemieux P, Vinogradov S, Alakhov V. Adv Drug Delivery Rev 2002;54:223–33.
[18] Kabanov AV, Batrakova EV, Alakhov VY. J Controlled Release 2002;82: 189–212.
[19] Yi X, Batrakova E, Banks WA, Vinogradov S, Kabanov AV. Bioconjugate Chem 2008;19:1071–7.
[20] Gaymalov ZZ, Yang Z, Pisarev VM, Alakhov VY, Kabanov AV. Biomaterials 2009;30:1232–45.
[21] Wang YQ, Su YL, Sun Q, Ma XO, Ma XC, Jiang ZY. J Membr Sci 2006;282:44–51.
[22] Oh SH, Kim JH, Song KS, Jeon BH, Yoon JH, Seo TB, et al. Biomaterials 2008;29:1601–9.
[23] Shi Q, Ye SJ, Kristalyn C, Su YL, Jiang ZY, Chen Z. Langmuir 2008;24: 7939–46.
[24] Kiss E, Bertoti I, Vargha-Butler EI. J Colloid Interface Sci 2002;245:91–8.
[25] Park TG, Cohen S, Langer R. Macromolecules 1992;25:116–22.